





Strongly interacting two-dimensional electron systems: Evidence for enhanced one-dimensional edge-channel coupling

C. Marty ^{1,2,*} C. Reichl ^{1,2} S. Parolo,^{1,2} I. Grandt-Ionita ^{1,2,3} J. Scharnetzky,^{1,2} W. Dietsche,^{1,2,4} and W. Wegscheider ^{1,2}

¹Laboratory for Solid State Physics, ETH Zürich, CH-8093 Zürich, Switzerland

²Quantum Center, ETH Zürich, CH-8093 Zürich, Switzerland

³Institut für Nanostruktur-und Festkörperphysik, Universität Hamburg, D-22761 Hamburg, Germany

⁴Max-Planck-Institut für Festkörperforschung, D-70569 Stuttgart, Germany



(Received 18 July 2023; revised 27 October 2023; accepted 14 November 2023; published 11 December 2023)

We observe nearly vanishing Hall resistances for integer filling factors in a counterflow experiment on a density-balanced two-dimensional (2D) bilayer system. Filling-factor-dependent equilibration lengths demonstrate enhanced 1D coupling via edge channels. Due to the narrow barrier the edge modes of the two 2D electron gases are in close proximity allowing for exciton formation at the sample edges. Electron drag measurements confirm the observed quantum-state-selective coupling between the layers.

DOI: [10.1103/PhysRevB.108.235131](https://doi.org/10.1103/PhysRevB.108.235131)

I. INTRODUCTION

Semiconductor heterostructures formed by aluminium (Al), gallium (Ga), and arsenic (As) have outstanding material properties for the growth of high-mobility bilayers of two-dimensional electron gases (2DEGs) in close proximity. The bilayer coupling depends on the ratio between the intralayer and interlayer Coulomb forces, governed by the electron density and the center-to-center quantum well (QW) separation [1]. In addition, the Coulomb gap suppresses the tunneling of electrons between the layers for increasing perpendicular magnetic fields [2]. The interaction between adjacent two-dimensional (2D) charge layers leads to a multitude of phenomena. In zero magnetic field, the electron tunneling between similar 2DEGs shows a conductance resonance at equal densities and zero interlayer bias due to momentum and energy conservation [3–5]. In high magnetic fields where the energy levels of the charges are quantized in Landau levels (LLs), a charge condensate state can be observed if the sum of the LL fillings of the adjacent layers equals 1. In this case, vanishing Hall and longitudinal resistances in a counterflow (CF) experiment as well as quantized Coulomb drag are signatures of an exciton condensate [6–8]. The latter is made up of filled and empty electron states showing a BCS-like behavior interpreted as condensation of 2D excitons [9–14]. Dissipationless flow of the exciton condensate and the Josephson effect between the layers have been observed [15].

Similarly, we here present filling-factor-dependent vanishing Hall resistances in a CF experiment and nearly quantized Coulomb drag resistances for integer filling factors on a balanced-density 2DEG bilayer system in a strongly interacting regime. This filling-factor-dependent enhanced coupling is observed for single-layer filling factors $\nu \geq 2$. However, for integer filling factors the bulk of the 2DEG is in a localized state where the transport takes place in edge modes only.

The vanishing Hall resistances originate from equilibration of these edge modes at the edge of the sample through electron tunneling, rather than a correlated bulk phenomena reported on previously. This electron tunneling picture is consistent with our computed equilibration lengths between the edge channels of the two 2DEGs, which are strongly filling factor dependent. Our device distinguishes itself from the preceding reported research by exhibiting higher electron mobilities and enlarged tunneling coupling due to the 6-nm-thick barrier between the layers. Using ion-implanted back gates, we are able to measure both layers independently.

II. DEVICE FABRICATION AND CHARACTERIZATION

We establish patterned back gates by photolithography and oxygen ion implantation on a metal-organic chemical vapor deposition (MOCVD) prepared GaAs wafer [16]. Subsequently, the implanted wafer is overgrown by molecular beam epitaxy with an AlGaAs-GaAs heterostructure, featuring two GaAs QWs of 18.7 nm width and an Al_{0.8}Ga_{0.2}As barrier of 6 nm [16,17]. The QWs are remotely doped with silicon, enabling mobilities of $2 \times 10^6 \text{ cm}^2 \text{ V}^{-1} \text{ s}^{-1}$ in each QW at a single-layer density of $0.92 \times 10^{11} \text{ cm}^{-2}$.

A Hall bar of 1250 μm length and 200 μm width is photolithographically processed, as shown in Fig. 1. We use ion-implanted pinch-off back gates and metallic top pinch-off gates to contact the 2DEGs separately [17]. Global top and back gates are used to tune the upper and lower 2DEG densities, respectively.

By applying a sufficient negative back gate voltage the bottom 2DEG can be depleted of its charge carriers. Thereby, the top 2DEG's transport characteristics can be probed as a single layer. The density of the top layer predominantly depends on the top gate voltage and is independent of the lower 2DEG density. Analogously, the top 2DEG can be depleted, and the bottom QW can be characterized, as seen in Fig. 2(a). Typical quantum Hall resistances featuring plateaus at fractions of the von Klitzing constant are obtained [18], while the longitudinal

*Corresponding author: chmarty@ethz.ch

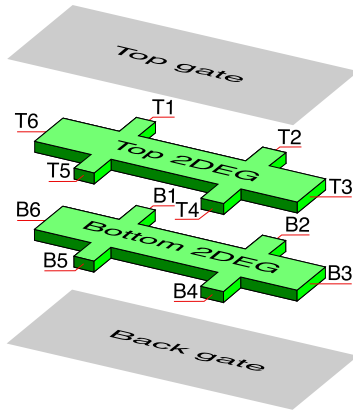


FIG. 1. Schematic of the bilayered Hall bars with contact labels.

resistance vanishes at integer fillings. Using this single-layer characterization technique, the gate voltages to balance the 2DEG densities can be determined.

By applying Fourier transform analysis to the Shubnikov-de Haas (SdH) oscillations the energy splitting Δ_{SAS} between the symmetric and antisymmetric wave functions can be

determined [19], which for our sample yields a value of $\Delta_{\text{SAS}} \approx 160 \mu\text{eV}$ (see Supplemental Material [20]).

The zero-bias tunneling conductivity can be determined by a differential conductance measurement. The zero-field conductivity is the largest and decreases strongly with applied perpendicular magnetic field, ranging from 19 mS at low field to below 1 mS at high field [20].

III. COUNTERFLOW AND DRAG EXPERIMENTS

In our CF experiment a current of 1 nA is fed into the top 2DEG (contact T6) and is drawn from the bottom 2DEG (contact B6). A wire connects the far end of the two Hall bars (contacts T3 and B3). The gates are adjusted such that both 2DEGs have the same density of $0.92 \times 10^{11} \text{ cm}^{-2}$.

For a CF experiment with completely uncoupled QWs, one would expect the Hall resistivities in the individual layers to coincide with those traditionally observed in a single layer. If, however, the QWs are strongly coupled, meaning that charges can be exchanged readily, then the Hall voltages would compensate each other to zero. The coupling between the two layers and, in turn, the tunneling conductivity depend on the center-to-center QW distance, the barrier width, and

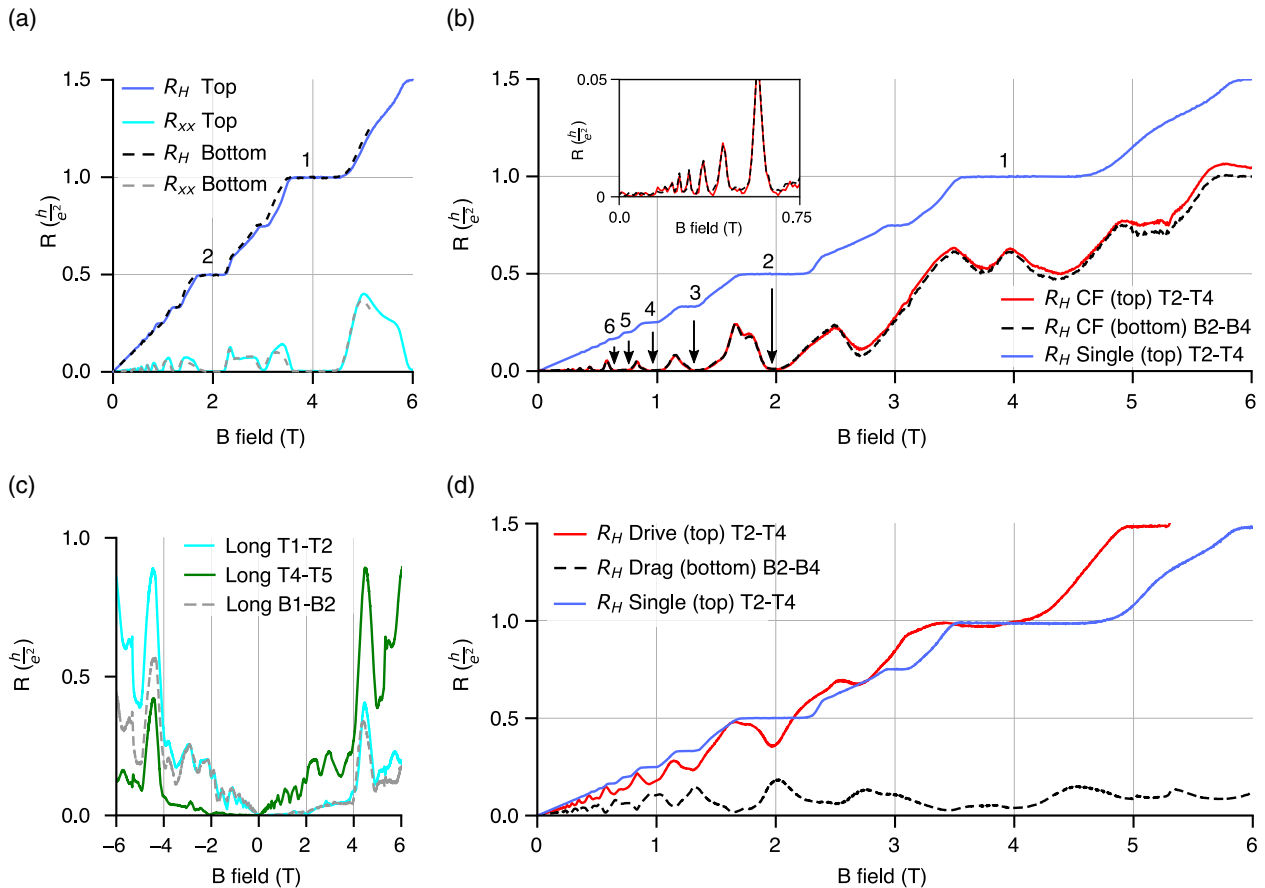


FIG. 2. (a) Individually recorded Hall and longitudinal resistances for the top and bottom 2DEGs. (b) The Hall resistances for both layers in the CF experiment nearly vanish for the same integer fillings. For higher magnetic fields the CF Hall resistance increases. Inset: CF Hall resistances for small fields. (c) The CF longitudinal resistance is asymmetric in magnetic field. The resistances on the same side of the Hall bar are alike. (d) Drag experiment: The Hall resistance of the current-carrying top layer roughly follows the single-layer Hall resistance trace. Minima occur at integer filling factors where the drag resistance in the bottom layer features a maximum. The drag resistance does not have a maximum at $\nu = 1$.

the applied magnetic field. In our sample the tunneling area of 0.25 mm^2 results in a tunneling conductivity as high as 19 mS for small perpendicular magnetic fields and lower for higher fields. Hence, for a CF Hall resistance at small fields, a strongly reduced Hall resistance due to electron tunneling is expected. For high magnetic fields where the Coulomb gap suppresses tunneling, a resistance closer to the single-layer resistance has to be anticipated. For our CF Hall resistance measurement we measured the Hall resistance in both layers simultaneously between contacts T2 and T4 and contacts B2 and B4. In Fig. 2(b) the CF Hall resistances are compared with the single-layer Hall resistance with labeled integer filling factors. We record Hall resistances remaining below 100Ω for magnetic fields up to 0.2 T . From 0.2 T on until 2.2 T the Hall resistance increases and features filling-factor-dependent minima smaller than 270Ω . For filling factors lower than $\nu < 2$ the CF Hall resistance does no longer nearly vanish.

Longitudinal resistance voltage measurements for the CF experiment display a pronounced magnetic field sign dependence, as seen in Fig. 2(c). Either the longitudinal resistance increases with magnetic field as $1/B$ periodic SdH oscillations or it is nearly zero depending on the sign of the magnetic field. The longitudinal resistance near zero field ($0 \pm 0.2 \text{ T}$) is roughly 25Ω , which is smaller than the corresponding single-layer longitudinal resistance. This indicates that a large portion of the current tunnels between the 2DEGs for such small fields. In this magnetic field range the experiment does not resemble a CF experiment.

Similarly to the longitudinal resistance, the interlayer voltage features a strong magnetic-field-dependent asymmetry, as seen in Fig. 3(a). The interlayer voltage is composed of either twice the Hall voltage or zero voltage. Whether the voltage is zero or corresponds to twice the Hall voltage depends on the side of the Hall bar. For nonzero potentials the voltage difference follows the same oscillatory maxima and minima as the Hall resistance. Comparing the interlayer voltages on the same side shows that for contacts closer to the current driving (contact T6) and the ground lead (contact B6) a larger voltage is measured.

The magnitude of the coupling between the two layers leads to a Coulomb drag response [8]. For our drag experiment a constant drive current of 1 nA is passed through the top 2DEG from contact T6 to contact T3, and we measure the Hall resistance in both layers (contacts T2 and T4 and contacts B2 and B4). In Fig. 2(d) we compare the single-layer Hall resistance of the current-carrying top layer and the drag resistance in the lower 2DEG. The top layer follows the single-layer trace. At integer fillings the resistance drops substantially. For the electron-populated but nondriven bottom layer the Hall resistance also increases with magnetic field, with distinctive maxima at integer filling factors. The relative magnitude of the resistance of the bottom layer compared with the top layer indicates the coupling strength between the layers. The locations of the maxima coincide with the minima of the vanishing Hall resistances measured in the CF experiment.

IV. EQUILIBRATING EDGE CHANNELS

Condensation of the 2DEGs' density of states for a perpendicular magnetic field into LLs can be described by the

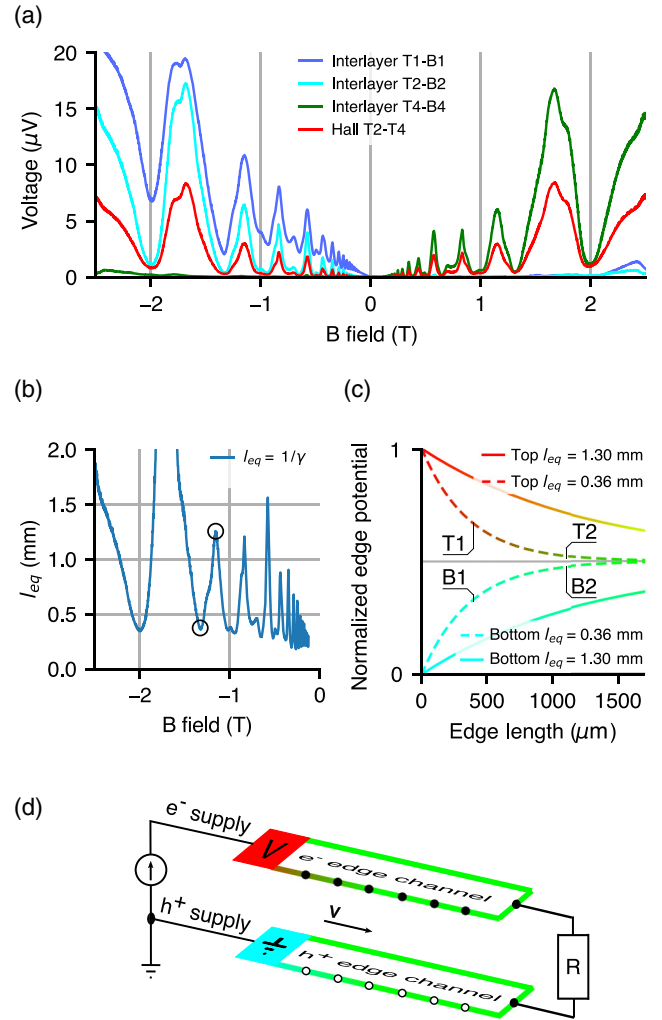


FIG. 3. (a) Interlayer voltages are strongly asymmetric. For the nonvanishing side, the interlayer voltage is twice the Hall voltage. The interlayer voltage features the same minima as the Hall voltage. (b) Calculated equilibration length l_{eq} using the interlayer voltages from one side of the sample are depicted. The equilibration lengths for two fillings, $\nu = 3$ and $\nu = 3.5$, are circled. (c) Using the circled equilibration lengths, 0.36 mm and 1.3 mm potentials for the top and the bottom edge channels are computed. (d) Simplified schematic of the Hall bar-shaped edge modes for a CF experiment.

Büttiker 1D edge-channel picture [21]. When the bulk of the sample is in an insulating gapped state, corresponding to the Fermi level being between two LLs, only the chiral edge modes carry current. An applied bias offsets the Fermi levels slightly and leads to a net current. In this situation the electron density is increased on one side of the sample and lowered on the other. The density reduction is equivalent to a population with holes.

In the special case of a CF experiment, the electron density increase in the top layer is situated above the augmented hole population in the bottom layer, as illustrated in Fig. 3(d). This applies for both sides of the Hall bar. As the excitonic binding energy of electrons and holes in one dimension is strongly enhanced in contrast to its counterpart for bulk 2D excitons

[22,23], we also expect increased tunneling between the 1D edge channels.

Figure 2(b) shows that the Hall resistance nearly vanishes in both layers for an insulating bulk. For the Hall resistance to vanish, the potentials across the Hall bars must be equal. This charge balancing cannot take place in the insulating bulk of the sample. In addition, the recorded interlayer voltage is minimal for the same filling factors ν as the Hall resistance. Therefore the potentials are nearly the same in both 2DEGs. The Coulomb gap suppresses electron tunneling in the bulk leaving the equilibration of the potentials to the edges. We suggest that the equilibration of the edge modes at integer filling factors leads to the almost complete vanishing of the Hall resistances observed in the CF experiment.

Equilibration between the edge modes is established by electron tunneling. A shorter equilibration length relates to an increased coupling between the two 2DEGs. In Fig. 2(d) the drag resistance features distinctive maxima for integer filling factors $\nu \geq 2$ where the current-driven top 2DEG shows minima. The increase (decrease) in Hall voltage is caused by an increased (decreased) current in the bottom (top) 2DEG caused by electron tunneling. We suspect that tunneling occurs predominantly between edge channels, where occupied conduction band states are positioned above unoccupied states in close proximity. The electrons in the bulk are localized, and there are no unoccupied states. The highest tunneling coupling is achieved at integer filling factors.

V. CALCULATING THE EQUILIBRATION LENGTH

Equilibration between adjacent edge modes by tunneling has been discussed before [24]. Coupled differential rate equations yield an equation for the potential difference between the channels

$$\mu_1(x) - \mu_2(x) = e^{-\gamma x}[\mu_1(0) - \mu_2(0)], \quad (1)$$

where γ is the equilibration rate describing the electron tunneling probability per length. The characteristic equilibration length is then defined by $l_{\text{eq}} = 1/\gamma$.

For our bilayer system the left-hand side of Eq. (1) is the measured interlayer voltage at a distance x . The right-hand side is the initially applied bias times an exponential decay factor depending on the length of copropagation of the edge channels. We use Eq. (1) and the measured interlayer voltages between contacts T1 and B1 and between contacts T2 and B2 from Fig. 3(a) to calculate the equilibration length in our CF experiment. The distance between contact T1 and contact T2 is approximately equal to 650 μm . The equilibration lengths are plotted in Fig. 3(b). Using the equilibration lengths of 360 and 1300 μm , normalized edge potentials were calculated with Eq. (1) and are depicted in Fig. 3(c). The exponential decay (increase) of the potential along the top (bottom) edge represents a consistent description of the measured CF voltages. From Fig. 3(c) the interlayer voltage is directly obtained by choosing a distance from the origin and taking the difference between the top and bottom potentials. The Hall voltage is determined by taking the difference between the computed potential and half of the applied voltage. Finally, the longitudinal voltage is obtained by computing the potential drop between two points on the x axis.

From the computed edge-channel potentials of Fig. 3(c) the asymmetric behavior of the interlayer voltages and the longitudinal resistances becomes evident. The edge modes on one side of the sample have equilibrated to half of the applied potential. Hence the longitudinal voltage and the interlayer voltage are minimal on that side. With a change in chirality the opposing side of the Hall bar then measures zero-potential difference. The nearly vanishing Hall resistance is a consequence of the decreased equilibration length between the edge modes.

As described before, exciton formation between the 1D edge channels can be responsible for an enhanced coupling at integer filling factors and an almost complete vanishing of the Hall, longitudinal, and interlayer voltages. Since for completely filled LLs, where the bulk is insulating, electronic transport exclusively takes place along the sample edges, 1D exciton formation there has the strongest effect on tunneling.

Strikingly, our picture does not apply to the filling factor $\nu = 1$. The spin-polarized filling factor $\nu = 1$ is different. Around $\nu = 1$, skyrmionic ground states consisting of charged spin textures affect the tunneling between the layers leading to an increase in equilibration length [25,26]. As seen in Fig. 2(b) the Hall resistance does not vanish at filling factor $\nu = 1$. The plateaus at fractions of the von Klitzing constant are present and less pristine. The curve seems to be shifted by the magnetic field corresponding to the filling of $\nu = 2$. The drag resistance in Fig. 2(d) shows no maxima at filling factor $\nu = 1$; this is compliant with the nonvanishing Hall voltage. The coupling between the two layers remains low for fillings $\nu < 2$. Additionally, the longitudinal resistance partly loses its asymmetry for $\nu < 2$. Therefore the edge channels do not equilibrate, which is consistent with a longitudinal resistance measured on both sides of the Hall bar. Tunneling experiments for fillings below $\nu < 2$ must, thus, be described differently.

Finally, we do not expect to observe a bulk Bose-Einstein condensate (BEC) with vanishing Hall voltages at filling $\nu = 1/2$ in our counterflow measurement. For our sample the ratio $\Delta_{\text{SAS}}/(e^2/(4\pi\epsilon_0 l_B))$ is approximately equal to $12.6e^{-3}$. The condition for a BEC to form in this case is $d/l_B < 2$, which is substantially smaller than our value of 2.65 at 8 T ($\nu = 1/2$).

VI. CONCLUSIONS

In conclusion, we widen the observable parameter space by investigating a high-mobility sample with a 6-nm barrier and independent contacts to each layer. In our CF experiment we explore the transition between strong and weak couplings of the QWs, where potential equalization takes place through tunneling between the chiral edge modes of the QWs. We observe nearly vanishing Hall resistances at integer filling factors $\nu > 1$. We trace the selectiveness of the equilibration to the enhanced tunneling coupling at filled LLs, which corresponds to a merging of occupied and unoccupied electron states in close proximity at the edge. The increased coupling originates from the excitonic binding between the electrons and holes in the one-dimensional edge modes. With the currently realized sample design allowing for independent contacts to strongly coupled bilayer systems, investigations into couplings between different filling factors or fractional edge modes become feasible.

ACKNOWLEDGMENTS

We thank Thomas Ihn, Filip Krizek, and Ady Stern for illuminating discussions. We acknowledge financial support

from the Swiss National Science Foundation (SNSF) and the NCCR QSIT (National Center of Competence in Research - Quantum Science and Technology).

-
- [1] S. Q. Murphy, J. P. Eisenstein, G. S. Boebinger, L. N. Pfeiffer, and K. W. West, Many-body integer quantum Hall effect: Evidence for new phase transitions, *Phys. Rev. Lett.* **72**, 728 (1994).
- [2] J. P. Eisenstein, L. N. Pfeiffer, and K. W. West, Coulomb barrier to tunneling between parallel two-dimensional electron systems, *Phys. Rev. Lett.* **69**, 3804 (1992).
- [3] J. P. Eisenstein, New transport phenomena in coupled quantum wells, *Superlattices Microstruct.* **12**, 107 (1992).
- [4] T. Jungwirth and A. H. MacDonald, Tunneling between parallel two-dimensional electron liquids, *Surf. Sci.* **361-362**, 167 (1996).
- [5] D. C. Tsui, H. C. Manoharan, and M. Shayegan, Observation of an abrupt double-to-single-layer transition in a double-quantum-well structure, *Surf. Sci.* **305**, 405 (1994).
- [6] M. Kellogg, J. P. Eisenstein, L. N. Pfeiffer, and K. W. West, Vanishing Hall resistance at high magnetic field in a double-layer two-dimensional electron system, *Phys. Rev. Lett.* **93**, 036801 (2004).
- [7] M. Kellogg, I. B. Spielman, J. P. Eisenstein, L. N. Pfeiffer, and K. W. West, Observation of quantized Hall drag in a strongly correlated bilayer electron system, *Phys. Rev. Lett.* **88**, 126804 (2002).
- [8] X. Liu, K. Watanabe, T. Taniguchi, B. I. Halperin, and P. Kim, Quantum Hall drag of exciton condensate in graphene, *Nat. Phys.* **13**, 746 (2017).
- [9] J. P. Eisenstein and A. H. MacDonald, Bose-Einstein condensation of excitons in bilayer electron systems Bose-Einstein condensation of excitons in bilayer, *Nature (London)* **432**, 691 (2004).
- [10] I. B. Spielman, J. P. Eisenstein, L. N. Pfeiffer, and K. W. West, Resonantly enhanced tunneling in a double layer quantum Hall ferromagnet, *Phys. Rev. Lett.* **84**, 5808 (2000).
- [11] E. Tutuc, M. Shayegan, and D. A. Huse, Counterflow measurements in strongly correlated GaAs hole bilayers: Evidence for electron-hole pairing, *Phys. Rev. Lett.* **93**, 036802 (2004).
- [12] L. Tiemann, Y. Yoon, W. Dietsche, K. von Klitzing, and W. Wegscheider, Dominant parameters for the critical tunneling current in bilayer exciton condensates, *Phys. Rev. B* **80**, 165120 (2009).
- [13] X. Liu, J. I. A. Li, K. Watanabe, T. Taniguchi, J. Hone, B. I. Halperin, P. Kim, and C. R. Dean, Crossover between strongly coupled and weakly coupled exciton superfluids, *Science* **375**, 205 (2022).
- [14] Q. Shi, E.-M. Shih, D. Rhodes, B. Kim, K. Barmak, K. Watanabe, T. Taniguchi, Z. Papic, D. A. Abanin, J. Hone, and C. R. Dean, Bilayer WSe₂ as a natural platform for interlayer exciton condensates in the strong coupling limit, *Nat. Nanotechnol.* **17**, 577 (2022).
- [15] M. Fogler and F. Wilczek, Josephson effect without superconductivity: Realization in quantum Hall bilayers, *Phys. Rev. Lett.* **86**, 1833 (2001).
- [16] M. Berl, L. Tiemann, W. Dietsche, H. Karl, and W. Wegscheider, Structured back gates for high-mobility two-dimensional electron systems using oxygen ion implantation, *Appl. Phys. Lett.* **108**, 132102 (2016).
- [17] J. Scharnetzky, J. Meyer, M. Berl, C. Reichl, L. Tiemann, W. Dietsche, and W. Wegscheider, A novel planar back-gate design to control the carrier concentrations in GaAs-based double quantum wells, *Semicond. Sci. Technol.* **35**, 085019 (2020).
- [18] K. v. Klitzing, G. Dorda, and D. M. Pepper, New method for high-accuracy determination of the fine-structure constant based on quantized Hall resistance, *Phys. Rev. Lett.* **45**, 494 (1980).
- [19] I. Lo, J. K. Tsai, W. J. Yao, P. C. Ho, L.-W. Tu, T. C. Chang, S. Elhamri, W. C. Mitchel, K. Y. Hsieh, J. H. Huang, H. L. Huang, and W. C. Tsai, Spin splitting in modulation-doped Al_xGa_{1-x}N/GaN heterostructures, *Phys. Rev. B* **65**, 161306(R) (2002).
- [20] See Supplemental Material at <http://link.aps.org/supplemental/10.1103/PhysRevB.108.235131> for the measured Hall voltage of the top (bottom) 2DEG depending on the applied top (back) gate voltage; the electron density of the top 2DEG; a SdH measurement of the top 2DEG; the Fourier transform of the SdH measurement; and differential tunnel conductance measurements at various perpendicular magnetic fields.
- [21] M. Büttiker, Absence of backscattering in the quantum Hall effect in multiprobe conductors, *Phys. Rev. B* **38**, 9375 (1988).
- [22] G. Bastard, E. E. Mendez, L. L. Chang, and L. Esaki, Exciton binding energy in quantum wells, *Phys. Rev. B* **26**, 1974 (1982).
- [23] I. V. Bondarev, Asymptotic exchange coupling of quasi-one-dimensional excitons in carbon nanotubes, *Phys. Rev. B* **83**, 153409 (2011).
- [24] G. Nicoli, C. Adam, M. Rössli, P. Märki, J. Scharnetzky, C. Reichl, W. Wegscheider, T. M. Ihn, and K. Ensslin, Spin-selective equilibration among integer quantum Hall edge channels, *Phys. Rev. Lett.* **128**, 056802 (2022).
- [25] S. L. Sondhi, A. Karlhede, S. A. Kivelson, and E. H. Rezayi, Skyrmions and the crossover from the integer to fractional quantum Hall effect at small Zeeman energies, *Phys. Rev. B* **47**, 16419 (1993).
- [26] J. G. Groshaus, V. Umansky, H. Shtrikman, Y. Levinson, and I. Bar-Joseph, Absorption spectrum around $\nu = 1$: Evidence for a small-size skyrmion, *Phys. Rev. Lett.* **93**, 096802 (2004).